



TECHNICAL UNIVERSITY OF CLUJ-NAPOCA

ACTA TECHNICA NAPOCENSIS

Series: Applied Mathematics, Mechanics, and Engineering  
Vol. 65, Issue Special IV, December, 2022

## FINITE ELEMENT MODELING OF DROPLET IMPACT ON SURFACES WITH DIFFERENT WETTABILITY AND MORPHOLOGY

Dimitrios SKONDRAS-GIOUSIOS, Marina GOUNARI, Maria BALANOU,  
Angelos P. MARKOPOULOS

**Abstract:** The manipulation of droplet impact on manufactured surfaces is of great importance for surface engineering applications related with anti-corrosion, self-cleaning, heat exchange and anti-icing properties. In this work, finite element analysis was utilized for creating computational models for studying the influence that different dynamic wetting states, surface morphologies and droplet velocities had on the droplet impact on the surface. A laminar two-phase flow model coupled with phase field or level set method was employed for capturing the droplet movement, using adaptive mesh refinement. The results showed that surface hydrophobicity/philicity as well as morphology have a significant influence on non-dimensional parameters such as spreading factor and apex height of the droplet as well as on breakage or bouncing of the droplet.

**Key words:** finite element modeling, phase-field method, droplet impingement, contact angle, surface roughness surface wettability

### 1. INTRODUCTION

In the last decades, the dynamics of droplet impacting on hydrophobic surfaces have attracted the interest of many researchers and happen in many industrial processes, some of them are inkjet printing, spray drying, spray cooling, 3D printing, anti-icing, etc. [1]. The results of droplet impact are influenced by the impact of the velocity of the droplet, droplet size, properties of the liquid, interfacial tension, wettability of the surface, and surface morphology (surface roughness) [2,3]. The impact of a droplet on hydrophobic surface results in different outcomes, such as partial or total spreading, recoil, or rebound [1].

Many studies have been carried out to study the droplet impact, based on the Wenzel model and Cassie–Baxter model [4-6]. According to the Wenzel model (or “homogenous wetting state”), the droplet penetrates the surface structure, meanwhile in the case of Cassie–Baxter model (or “heterogenous model state”), the droplet remains on the top of the surface structure, and

the air will be trapped in the space of the surface structure [7].

However, the theoretical models of Wenzel and Cassie–Baxter are not enough to study complex phenomena. For this reason, numerical models have been proposed to study the wettability of a hydrophobic surface. In more details, the dual-grid level-set method (DGLSM) used by Patil *et al.* [8] for modeling contact line motion. Furthermore, Sun *et al.* [9] used the three-dimensional volume of fluid (VOF) method to study the influence of droplet impact velocity, surface wettability, surface tension on the dynamics of the droplets on the surface morphology, and as well as the internal velocity and the pressure distribution. Li and Zhang [3] used Molecular Dynamic (MD) simulation to design a three-dimensional physical model of a nanodroplet on a superhydrophobic nano-pillared surface. Also, they investigated the contact time via different impact velocities and the effect of impact velocity on the contact diameter and restitution coefficient. Dalgamoni and Yong [10] used the lattice Boltzmann method (LBM) to investigate the physics of droplet impact on

spherical surfaces with different surface wettability and Weber number. Recently, phase-field (PF) method based on Cahn–Hilliard equation has come out as a suitable tool in modeling multiphase flows including the study of the wetting behavior of hydrophobic surfaces. In the PF method, based on the free-energy mode, an interface is reported as a finite volumetric transition zone across which physical properties differs [11]. PF model used by Zhang *et al.* [12] to study the effect of the Reynolds number, Weber number, density ratio, viscosity ratio, and the equilibrium contact angle (CA) of the solid surface in the dynamics of a droplet impacting on a flat solid surface. Moreover, a modified PH three-dimensional model developed by Shen *et al.* [13] to model the spreading of an impacting droplet, and the effect of thermal contact resistance on the maximum spread factor of a solidifying droplet was referred. The major advantage of PF method is that it allows the contact line of a droplet to move along the wetted surface [14]. In addition, compared with other numerical model methods is found to be less sensitive to numerical parameters, and as a result more stable [15]. In this work, dynamic droplet impact is studied on surfaces with different static characteristics involving the surface roughness, the CA or dynamic characteristics involving the impact droplet velocity, using PF method. The effect that surface hydrophobicity/philocity combined with various surface morphologies had on parameters related to surface wetting was examined.

## 2. METHODOLOGY

A 2D axisymmetric finite element method was implemented for the modeling and simulation of the impact of a water droplet to surfaces with different morphologies. In this section, comprehensive details on aspects such as geometry and physics modeling, mesh selection and solver configurations, which were used in the current study, are analyzed.

### 2.1 Geometry, material and physics modeling

The geometry of the model is a simple configuration of a water droplet surrounded by

air, over a surface, as seen in figure 1. In the initial configuration, droplet begins to fall with an initial velocity  $u_0$  from a distance  $h$  to the surface. The scale of geometry is in mm.

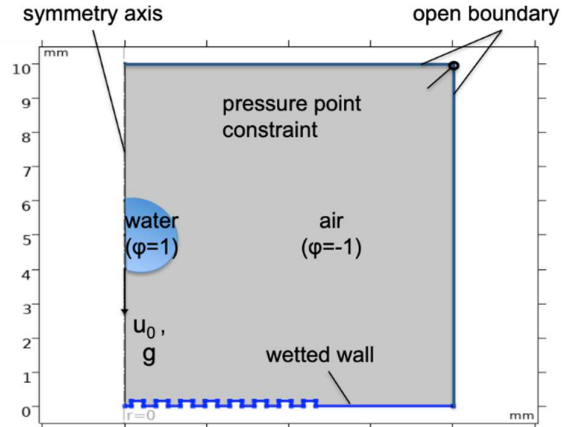


Fig. 1. Schematic model illustration.

The cross section of surfaces that were used for the simulations was rectangular, hemispherical or inverse trapezoidal. The fluids used for the simulations were water and air, with basic properties shown at table 1. Basic assumptions taken into account concerning the physics modeling stage were:

- Water droplet is considered a continuous, Newtonian and incompressible fluid.
- The field is assumed irrotational.
- Gravitational forces are included.
- No slip is occurring during fluid-wall contact.
- Flow is occurring isothermally without droplet condensation.

Table 1

Fluid	Fluid properties.		
	Density ( $\rho$ ) [kg/m <sup>3</sup> ]	Dynamic viscosity ( $\mu$ ) [Pa*s]	Surface tension ( $\sigma_{wa}$ ) [N/m]
Water	998	1e-3	0.072
Air	1225	1.81e-5	

The flow was modeled as a two-phase laminar flow, due to turbulence absence and low Re number in the real case scenario. Reference temperature ( $T_{ref}$ ) and pressure ( $P_{ref}$ ) are considered 293.15 K and 1 atm, respectively. Open boundary and pressure point constraint were utilized as boundary conditions for air, in

order to more realistically represent the vastness of air as well as to avoid unnatural pressure concentrations. Water droplet had an initial velocity value ranging from 0.05 m/s to 1.1 m/s.

The interface interaction was modeled via the PF method, where a function  $\varphi$  [-1,1] is used for the representation of two phases, as seen in figure 1. The phase separation is governed by the Cahn-Hilliard equation in its non-conservative form:

$$\frac{\partial \varphi}{\partial t} + u \nabla \varphi = \nabla \frac{\gamma \lambda}{\varepsilon^2} \nabla \psi \quad (1)$$

$$\psi = -\nabla \varepsilon^2 \nabla \varphi + (\varphi^2 - 1) \varphi + \frac{\varepsilon^2}{\lambda} \frac{\partial f_{ext}}{\partial \varphi} \quad (2)$$

where  $u$  is the velocity of fluid  $\psi$  is the PF help variable,  $\lambda$  is the mixing energy density,  $\gamma$  is the mobility parameter,  $\varepsilon$  is a capillary width that scales with the interface thickness and  $f_{ext}$  is the force arising due to external free energy, which in this case is 0. The most critical computational parameters affecting the realistic and robust representation of the droplet impact on a surface were found to be the parameter controlling interface thickness  $\varepsilon$  and the mobility tuning parameter  $\gamma$ . Test simulations showed that  $\varepsilon$  is more finely tuned when related with maximum element size ( $h_{max}$ ), and  $\gamma$  when related with initial velocity ( $u_0$ ) and interface tension ( $\sigma$ ):

$$\varepsilon = \frac{h_{max}}{2} \quad (3)$$

$$\gamma = \frac{4u_0}{3\sqrt{2}\sigma} \quad (4)$$

Wetting properties were defined explicitly, via CA between the two fluids. Here, different CA values simplistically represent the effect that lower scale roughness scales have on the apparent CA values, without actually modeling them. After the introduction of laminar two-phase flow and PF conditions, a physics coupling of those two is necessary, in order to properly track the movement and deformation of the interface between the phases of water and air. In addition, this multiphysics coupling enables the

inclusion of surface tension effects on the interface, during simulation.

## 2.2 Meshing and solver settings

Without the appropriate use of meshing settings, the derivation of realistic simulations is almost impossible to obtain. In order to reduce the computational cost without reducing the very dense mesh needed, an adaptive mesh refinement method was utilized. Adaptive mesh refinement makes the mesh finer in the moving fluid interface area during the time dependent solving procedure, as seen in figure 2. For the simulations triangular shaped elements were used, with a mean number of 40000 elements.

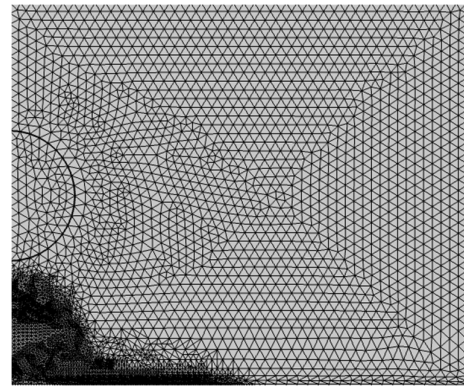


Fig. 2. Adaptive mesh refinement during simulation.

As mentioned before,  $h_{max}$  is crucial for obtaining the optimal interface thickness. This was certified with a parametric sweep of various  $h_{max}$  values, where an order of magnitude below  $10e-4$  proved to be significant for obtaining a satisfactory interface accuracy on the results of simulations, as seen in figure 3. The simulations ran using a time dependent solver, using backward differentiation formula (BDF) with phase initialization. An HP ProLiant DL380G7 server was used for the implementation of the simulations.

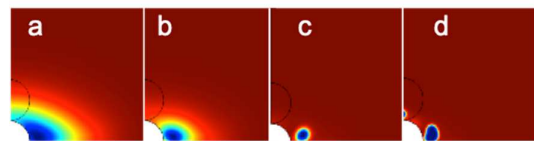


Fig.3. Interface results of the water (blue) and air (red) phase with different  $h_{max}$  values: a)  $4.5e-4$  m, b)  $3.6e-4$  m, c)  $1.7e-4$  m, d)  $8.7e-5$  m. Droplet radius is  $R=1.35$ mm.

## 3. RESULTS AND DISCUSSION

In this study, cases of water droplet impact on surfaces with various roughness profiles (flat, hemispherical, rectangular, and trapezoidal) and wetting properties (hydrophobic, hydrophilic) were considered. In some cases, the effect of initial velocity was also considered. The droplet impact results on surfaces were measured via the non-dimensional parameters spreading factor ( $\beta$ ) and apex height ( $h^*$ ) of droplet:

$$\beta = \frac{D_{max}}{D_0} \quad (3)$$

$$h^* = \frac{h_{max}}{D_0} \quad (4)$$

where  $D_{max}$  is the maximum spreading diameter of the droplet,  $D_0$  is the initial diameter of the droplet and  $h_{max}$  is the maximum vertical diameter of the droplet after impact. In some cases, non-dimensional time of droplet breakage initiation ( $t^*_{break}$ ) or time of droplet bounce initiation ( $t^*_{bounce}$ ) was used to describe the impact behavior.

$$t^* = t \frac{u_0}{D_0} \quad (5)$$

where  $\rho$  is fluid density,  $u$  is the droplet velocity,  $l$  is the characteristic length (droplet diameter) and  $\sigma$  is the fluid surface tension.

### 3.1 Droplet impact on flat surface

Initially, the droplet impact on a flat surface was considered. In order to validate the realistic capture of droplet dynamics of the model, droplet impact at three different Weber numbers [1.5, 33.5, 421] was considered, as in [16]. The droplet's morphological stages progression during impact showed satisfactory results especially for the two lower Weber numbers, as seen in figure 4, for the case of  $We = 33.5$ . A small rise in total contact time with  $We$  increase was also observed. The morphology of droplet bouncing stages was also in good accordance with [15]. The next step was the extraction of  $t^*_{break}$  for different wetting CA of droplet with  $R=1$  mm and  $u_0=1.1$  m/s, as seen in figure 5.

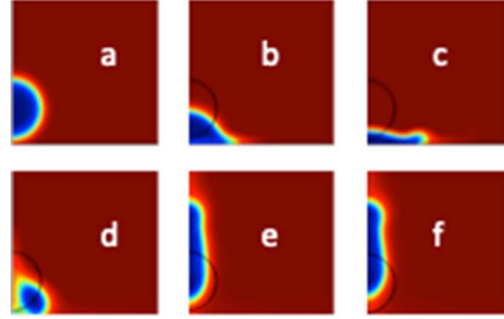


**Fig.4.** Stages of droplet ( $R=1.35$  mm) impact at  $We = 33.5$ : a) approach, b) impingement, c) spreading, d) break, e) retraction-bouncing, f) bouncing.

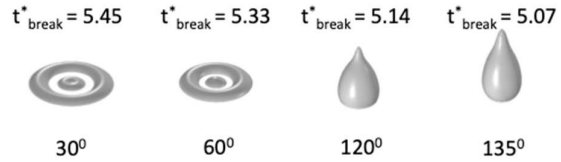


**Fig. 5.** Snapshots of droplets at  $t = 13.33$  ms for different CA.

A decreasing trend can be noticed, as CA increases.

However,  $t^*_{break}$  alone cannot fully depict the effect that CA has on droplet impact dynamics. It can be seen from figure 5 that at the same time, the water droplet had a completely different morphology in accordance to CA. When impacting on hydrophilic surfaces, water droplet is still in spreading and break phase. On the contrary, when impacting hydrophobic surfaces, water droplet is already on a retraction or bouncing phase.

### 3.2 Droplet impact on surface with local roughness

In this section, the droplet impingement on surfaces with local roughness, hemispherical or cylindrical, is studied. Again, changes in CA imply the existence of a second, smaller scale roughness. The morphology of droplet was again compared, for the hemispherical case, with the results of [17]. Snapshots of the simulation progress can be seen in figure 6. The ratio of the radius of the hemispherical superhydrophobic ( $163^\circ$ ) surface ( $R= 2.3$  mm) to the radius of the droplet was 1:2, with droplet having  $u_0 = 1$  m/s. For different CA with the same parameters as

before, the droplet impact response exhibits significant differences.

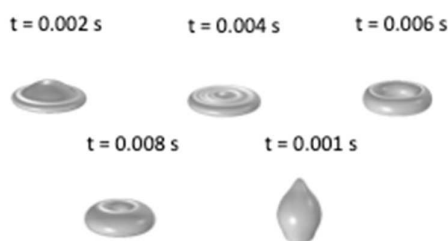


**Figure 1** Snapshots of simulation process for hemispherical local roughness with droplet hemisphere diameter ratio 1:2,  $u_0 = 1$  m/s and CA of  $163^\circ$ .

As seen in figure 7, when impacting the hydrophilic surface, the droplet fails to bounce and spreads without breaking or bouncing. On the contrary, when impacting the hydrophobic surface, a significant volume of droplet bounces back, after breakage. Subsequently, a cylindrical local roughness was tested. Here, droplet radius was same as in hemispherical case and  $u_0 = 0.05$  m/s. Again, different wetting characteristics had an important effect in the droplet impingement stages. As seen in figure 8, in the hydrophilic case, the water droplet broke after spreading, leaving a volume part under the cylinder. However, in the hydrophobic case, droplet managed to retract and stayed over the cylinder.

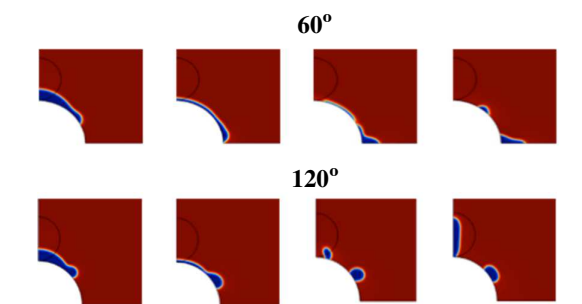


**Fig.7.** Snapshots for  $t=2, 4, 6$  and  $8$  ms of droplet impact on surface with hemispherical roughness of radius  $R=2.3$  mm and different wetting characteristics.



**Fig. 8.** Snapshots of droplet impact on surface with cylindrical roughness with cylinder radius of  $R=2.7$  mm and different wetting characteristics, for  $t = 0.05$  s and  $t = 0.1$  s.

Also, air entrapment was observed as in [18], for the hydrophobic case. The role that different surface wettability has on the dynamics of the impacting water droplet is also depicted in the non-dimensional parameters of table 2.

By making a surface from hydrophilic to hydrophobic affects spreading, maximum bounce and breakage time of droplet. More specifically, when surface was hydrophobic in both roughness types, spreading of droplet was decreased and droplet bouncing was increased, compared to hydrophilic cases. In addition, breakage time in hydrophobic surface had a small decrease in the hemispherical roughness case, while in cylindrical case no breakage occurred, compared to hydrophilic cases.

Moreover, the comparison between the two roughness profiles at hydrophobic states, showed that while the hemisphere type has slightly better dynamic response in terms of spreading and bouncing, in the cylindrical type no breakage occurred.

Table 2

**Comparison of droplet impact parameters between cylindrical and hemispherical roughness profiles.**

	Hydrophilic			Hydrophobic		
	$t^*_{break}$	$\beta_{max}$	$h^*_{max}$	$t^*_{break}$	$\beta_{max}$	$h^*_{max}$
	10.7	2.02	0.83	-	1.64	1.37
	2.53	2.9	1.54	2.27	1.09	2.78

### 3.3 Droplet impact on surface with extended roughness

In this section rectangular and inverse trapezoidal cross sections for extended roughness are tested. These surface morphologies are in general considered effective for many superhydrophobic applications.

In the rectangle profile case, the pillar-shaped protrusions had a square shape with a side of 0.09 mm with a distance  $d$  of 0.17 mm or 0.3 mm in some simulations. Water droplet had a radius  $R = 1$  mm and initial velocity of  $u_0 = 1$  m/s. In figure 9 snapshots of the droplet phases during impact on a superhydrophobic surface are depicted.

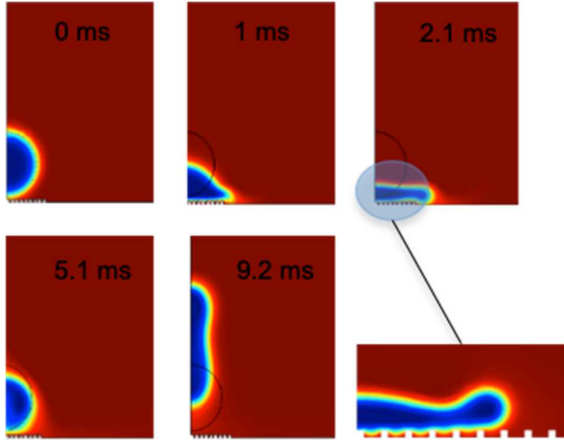


**Fig. 9.** Simulation snapshots for droplet ( $R=1$  mm) impact with superhydrophobic surface ( $155^\circ$ ).

Unlike most of the previous cases, no breakage of droplet is witnessed here. Absence of breakage is most likely to be attributed on the profile of the specific roughness, since in other cases with same initial values but other profiles droplet breakage occurred. Another interesting observation is that water does not penetrate at all inside the roughness cavities, like in Cassie-Baxter wetting regime. Consequently, the vast majority of surface area does not come in contact with water. This feature is considered desirable in non-wetting surface applications.

Compared with flat surface with the same initial parameter values, namely droplet radius, initial velocity and CA, rectangle profile surface roughness exhibited improved dynamic response in terms of reducing wetting.

According to table 3, total contact time ( $t_c$ ), moment of bounce ( $t_b$ ), spreading ( $\beta_{max}$ ) and maximum apex height ( $h^*_{max}$ ) are all improved when droplet impacts rectangle roughness profile, compared to flat surface.

When comparing two cases with the same roughness morphology, but with different distance between rectangle protrusions, namely  $d = 0.17$  mm and  $d = 0.3$  mm, the results are mixed. Greater protrusion distance results in less contact time smaller  $t_b$  and greater apex height. However, breaking of the droplet occurred. In contrast, smaller protrusion distance led to smaller droplet spreading and no droplet breakage occurred. The last surface morphology that was tested was a roughness with inverse trapezoidal cross section.

**Table 3**  
Comparison of droplet impact parameters between flat and rectangular roughness profile surfaces with CA of  $155^\circ$ .

	$t_c$ (ms)	$t^*_{break}$	$t_b$ (ms)	$\beta_{max}$	$h^*_{max}$
flat	7.2	5.1	9.2	2	1
rect- $d=0.17$	6.7	-	7.7	1.8	1.2
rect- $d=0.3$	4.6	3	5.1	1.9	2.6

Here, water droplet had a radius  $R = 2.7$  mm and initial velocity of  $u_0 = 1$  m/s. As seen before, a crucial anti wetting characteristic of surfaces with protrusion is the degree of liquid penetration in roughness cavities during contact with the liquid. At superhydrophilic CA ( $<30^\circ$ ) water was able to penetrate inside the cavities. However, even at hydrophilic CA ( $30^\circ - 90^\circ$ ) water did not penetrate cavities, as seen in figure 10, for the case of surface CA of  $60^\circ$ .

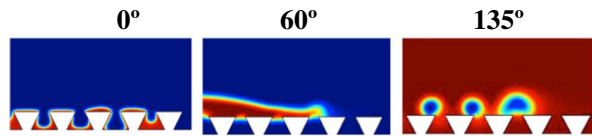


**Fig. 10.** Simulation snapshots of water droplet spreading for roughness with trapezoidal cross section, at different contact angles. Distance between the centers of two successive trapezoidal protrusions is 2mm.

The fact that even at hydrophilic states water is not able to wet the whole surface is an indicator of the importance role that roughness has on the wetting of surfaces. However, for the same roughness profile, the surface wettability affects spreading and breakage of droplet, according to table 4.

**Table 4**  
Droplet breakage time and spreading factor for impact at roughness with trapezoidal cross section at various CA

CA ( $^\circ$ )	$t^*_{break}$	$\beta_{max}$
45	5.6	2.9
60	5.9	2.9
120	6.2	2.8
150	6.6	2.6

For more hydrophobic surfaces, spreading of droplet tends to get restricted, as spreading factor decreases. On the contrary, non-dimensional breakage time increases with the increase of surface CA. Comparing the spreading results of tables 3 and 4 for roughness with rectangular and

trapezoidal cross sections, for the superhydrophobic surface cases, it can be deduced that at both rectangular profile roughness surfaces spreading of droplet is minimum. Moreover, when water droplet impacts the surface with trapezoidal cross section roughness has the maximum breakage time. Thus, larger surface portion is in contact with water for more time, compared with other surface morphologies, which is undesirable for anti-wetting applications.

#### 4. CONCLUSIONS

In this work, axisymmetric 2D finite element modeling of water droplet impact in surfaces with different morphologies and CA was implemented. The main purpose was to investigate the effect of different surface wettability regimes as well as different surface morphologies had during water droplet impact on them, in terms of droplet spreading, breaking, bouncing and portion of wetted surface. The results of flat and local roughness simulations were in agreement with similar computational or experimental setups from relevant literature. Consequently, other cases with different surface morphologies were examined.

One of the most important results was that in all cases considered, increased hydrophobicity of surfaces led to less droplet spreading and breakage times as well as increased height of droplet rebound. Additionally, it was observed that when roughness was superimposed with hydrophobicity, boosting of anti-wetting characteristics occurred in both rectangular and inverse trapezoidal roughness cross sections of surfaces. Moreover, simulations showed that among the tested surface morphologies, surface roughness with rectangular profile ( $d=0.3$ ) was considered as the most effective in terms of anti-wetting properties, such as minimum area of wetted surface, wetting time, droplet spreading and breakage time. Finally, when inverse trapezoidal profile was implemented, antiwetting properties were featured even at superhydrophilic CA, indicating the role of roughness in wettability.

Further research is encouraged to be conducted on more sophisticated dynamic contact angle models, more complicated roughness profiles (e.g., random roughness models) as well as on the effect of the surface slope on the dynamic droplet impact on surfaces, along with experimental validation of the above-mentioned cases.

#### 5. REFERENCES

- [1] Rioboo, R., Marengo, M., Tropea, C. *Time evolution of liquid drop impact onto solid, dry surfaces*. Exp Fluids, 33(1), 112-24, 2002, <https://doi.org/10.1007/s00348-002-0431-x>
- [2] Li, X., Fu, Y., Zheng, D., Fang, H., Wang, Y. *A numerical study of droplet impact on solid spheres: The effect of surface wettability, sphere size, and initial impact velocity*. Chem Phys, 550, 111314, 2021, <https://doi.org/10.1016/j.chemphys.2021.111314>
- [3] Li, H., Zhang, K. *Dynamic behavior of water droplets impacting on the superhydrophobic surface: Both experimental study and molecular dynamics simulation study*. Appl Surf Sci, 498(2), 143793, 2019, <https://doi.org/10.1016/j.apsusc.2019.143793>
- [4] Ebert, D., Bhushan, B. *Wear-resistant rose petal-effect surfaces with superhydrophobicity and high droplet adhesion using hydrophobic and hydrophilic nanoparticles*. J Colloid Interface Sci, 384(1), 182-8, 2012, <https://doi.org/10.1016/j.jcis.2012.06.070>
- [5] Zhang, B., Wang, J., Liu, Z., Zhang, X. *Beyond Cassie equation: Local structure of heterogeneous surfaces determines the contact angles of microdroplets*. Sci Rep, 4, 5822, 2014, <https://doi.org/10.1038/srep05822>
- [6] Marmur, A. *Wetting on hydrophobic rough surfaces: To be heterogeneous or not to be?* Langmuir, 19(20), 8343-8, 2003, <https://doi.org/10.1021/la0344682>
- [7] Elzaabalawy, A., Meguid, S.A. *Advances in the development of superhydrophobic and icephobic surfaces*. Int J Mech Mater Des, 18(3), 509-47, 2022, <https://doi.org/10.1007/s10999-022-09593-x>
- [8] Patil, N.D., Gada, V.H., Sharma, A., Bhardwaj, R. *On dual-grid level-set method for contact line modeling during impact of a*

- droplet on hydrophobic and superhydrophobic surfaces.* Int J Multiph Flow, 81, 54-66, 2016, <https://doi.org/10.1016/j.ijmultiphaseflow.2016.01.005>
- [9] Sun, J., Liu, Q., Liang, Y., Lin, Z., Liu, C. *Three-dimensional VOF simulation of droplet impacting on a superhydrophobic surface.* Biodes Manuf, 2(1), 10-23, 2019, <https://doi.org/10.1007/s42242-019-00035-w>
- [10] Dalgamoni, H.N., Yong, X. *Numerical and theoretical modeling of droplet impact on spherical surfaces.* Phys Fluids, 33(5), 2021, <https://doi.org/10.1063/5.0047024>
- [11] Takada, N., Tomiyama, A. *Numerical simulation of isothermal and thermal two-phase flows using phase-field modeling.* Int J Mod Phys C, 18(04), 536-45, 2007, <https://doi.org/10.1142/S0129183107010772>
- [12] Zhang, Q., Qian, T.Z., Wang, X.P. *Phase field simulation of a droplet impacting a solid surface.* Phys Fluids, 28(2), 2016, <https://doi.org/10.1063/1.4940995>
- [13] Shen, M., Li, B.Q., Yang, Q., et al. *A modified phase-field Three-dimensional model for droplet impact with solidification.* Int J Multiph Flow, 116, 51-66, 2019, <https://doi.org/10.1016/j.ijmultiphaseflow.2019.04.004>
- [14] Lim, C.Y., Lam, Y.C. *Phase-field simulation of impingement and spreading of micro-sized droplet on heterogeneous surface.* Microfluid Nanofluid, 17(1), 131-48, 2014, <https://doi.org/10.1007/s10404-013-1284-8>
- [15] Xiong, X., Wan, K.T., Hu, J., Xiao, H. *Effects of Contact Angle on the Dynamics of Water Droplet Impingement.* In Proceedings of the COMSOL Conference, 2015, <https://www.researchgate.net/publication/283570460>
- [16] Qu, J., Yang, Y., Yang, S., Hu, D., Qiu, H. *Droplet impingement on nano-textured superhydrophobic surface: Experimental and numerical study.* Appl Surf Sci, 491, 160-70, 2019, <https://doi.org/10.1016/j.apsusc.2019.06.104>
- [17] Bordbar, A., Taassob, A., Khojasteh, D., Marengo, M., Kamali, R. *Maximum spreading and rebound of a droplet impacting onto a spherical surface at low Weber numbers.* Langmuir, 34, 5149-58, 2018, <https://doi.org/10.1021/acs.langmuir.8b00625>
- [18] Ren, W., Foltyn, P., Geppert, A., Weigand, B. *Air entrapment and bubble formation during droplet impact onto a single cubic pillar.* Sci Rep, 11, 18018, 2021, <https://doi.org/10.1038/s41598-021-97376-3>

## MODELAREA CU ELEMENTE FINITE A IMPACTULUI UNEI PICĂTURI CU SUPRAFEȚELE CARACTERIZATE PRIN UMECTABILITATE ȘI MORFOLOGII DIFERITE

*Controlul impactului picăturilor cu suprafețele prelucrate este de mare importanță pentru aplicațiile din ingineria suprafețelor ce iau în considerare proprietățile lor anticorozive, de autocurățare, de schimb de căldură și de anti-înghețare. În această lucrare, a fost aplicată analiza cu elemente finite pentru crearea unor modele de calcul destinate studierii influenței pe care diferitele stări dinamice de umectare, diferitele morfologii de suprafață și diferitele viteze ale picăturilor le pot avea asupra impactului picăturii cu suprafața. A fost folosit un model de curgere laminară în două faze, cuplat cu metoda câmpului de fază sau cu metoda reglării nivelului, pentru obținerea de informații asupra mișcării picăturilor, folosind o rafinare adaptivă a rețelei. Rezultatele au arătat că hidrofobicitatea/hidrofilicitatea suprafeței, precum și morfologia acesteia, au o influență semnificativă asupra parametrilor non-dimensionali, așa cum sunt factorul de dispersie și înălțimea vârfului picăturii, precum și asupra ruperii sau stării picăturii.*

**Dimitrios SKONDRAS-GIOUSIOS**, Laboratory of Manufacturing Technology, School of Mechanical Engineering, National Technical University of Athens, diskogi@mail.ntua.gr, +302107723897, Heroon Polytecniou 9, 157 80, Athens, Greece

**Marina GOUNARI**, Laboratory of Manufacturing Technology, School of Mechanical Engineering, National Technical University of Athens, innamarina97@gmail.com, +302107723897, Heroon Polytecniou 9, 157 80 Athens, Greece

**Maria BALANOU**, Laboratory of Manufacturing Technology, School of Mechanical Engineering, National Technical University of Athens, mpalanoumaria23@mail.ntua.gr, +302107723897, Heroon Polytecniou 9, 157 80 Athens, Greece

**Angelos P. MARKOPOULOS**, Associate Professor, Laboratory of Manufacturing Technology, School of Mechanical Engineering, National Technical University of Athens, amark@mail.ntua.gr, +302107724299, Heroon Polytecniou 9, 157 80, Athens, Greece